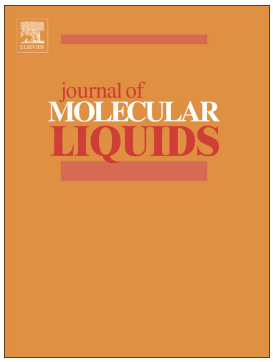


# Deciphering the anthelmintic activity of benzimidazolium salts by experimental and in-silico studies

Prabodh Ranjan, Mohd Athar, Kari Vijayakrishna, L.K. Meena, R. Vasita, Prakash C. Jha

PII: S0167-7322(18)31195-4
DOI: doi:10.1016/j.molliq.2018.07.029
Reference: MOLLIQ 9350

To appear in: *Journal of Molecular Liquids*

Received date: 7 March 2018
Revised date: 21 June 2018
Accepted date: 8 July 2018

Please cite this article as: Prabodh Ranjan, Mohd Athar, Kari Vijayakrishna, L.K. Meena, R. Vasita, Prakash C. Jha , Deciphering the anthelmintic activity of benzimidazolium salts by experimental and in-silico studies. Molliq (2018), doi:10.1016/j.molliq.2018.07.029

# Deciphering the Anthelmintic Activity of Benzimidazolium salts by Experimental and *In-silico* Studies

Prabodh Ranjan[1], Mohd Athar[1], Kari Vijayakrishna[4], L.K. Meena[3], R. Vasita[3], Prakash C. Jha[2‡]

[1]CCG@CUG, School of Chemical Sciences, Central University of Gujarat, Sector-30, Gandhinagar-382030, Gujarat, India.

[2]CCG@CUG, Centre for Applied Chemistry, Central University of Gujarat, Sector-30, Gandhinagar-382030, Gujarat, India.

[3]School of Life Sciences, Central University of Gujarat, Sector-30, Gandhinagar-382030, Gujarat, India.

[4]Department of Chemistry, School of Advanced Sciences, VIT University, Vellore-632014, Tamil Nadu, India

To whom correspondence should be addressed: Dr. Prakash Chandra Jha, Centre for Applied Chemistry, Central University of Gujarat, Sector-30, Gandhinagar-382030, Tel.: +91 8866823510; E-mail: prakash.jha@cug.ac.in

ORCID: 0000-0002-1709-511X

**Abstract:**

Inspired from the facts that majority of the drug administrated in the form of salts and "*poison is in the dose*"; herein, we have synthesized and characterized 1-methyl-3-alkylbenzimidazolium and 1-methyl-3-alkylimidazolium derived ionic salts with varying N-alkyl chains and different anions. These ionic salts were evaluated for their vermicidal activity (VA) and cell viability test against the *Pheretima posthuma* and A549 cell lines (human alveolar basal epithelial cells), respectively. The morphological changes in the test organism were visualized by the Scanning Electron Spectroscopy (SEM) to get the mechanistic insight. Furthermore, results were compared with VA of 1-methyl-3-alkylimidazolium derivatives to establish their structure-activity-relationship (SAR) of the fused benzene ring in 1-methyl-3-alkylimidazolium. The current findings suggested that the activity of these salts depend on the nature of N-alkyl side-chain, anionic moieties, varying charge on quaternary nitrogen (due to different anions) lipophilicity and types of cationic core fused with imidazolium ring. These findings were complemented by the quantitative-structure-activity-relationship, molecular docking approaches to unfold the features accountable for their activities and binding patterns of the ligand-receptor complex respectively. ADME/T assessment of the ionic salts shows that all fifteen compounds qualified the ADMET profiling test (that means they exhibits drug-likeness features).

**Keywords:** Ionic Liquids, 1-methylbenzimidazolium, Vermicidal, *Pheretima posthuma* and Albendazole sulfoxide.

**Abbreviations**

| | |
|---|---|
| ILs | Ionic Liquids |
| ABZSO | Albendazole sulfoxide |
| SIFts | Structural Interaction Fingerprints |
| QSAR | Quantitative structure activity relationship |
| MLR | Multi Linear Regression |
| SEM | Scanning Electron Microscopy |

## 1. Introduction

Helminthic infections are neglected tropical diseases (NTDs), caused by helmintic worms (*e.g.*, tape worm, and hook worm etc.). These infections have affected a wide continuum of population in developing countries due to poor sanitations and lack of social awareness [1-8]. Measures have been taken to control and eradicates such infections by developing several drugs (*i.e.*, Benzimidazole carbamates (BZCs) derivatives, Levomesol, Paraziquintel, and Pyrental etc.) and by means of awareness programs [9-17]. Their poor bioavailability and excessive uses have led to drug resistance owing to evolutionary adaptations of helminths [10, 18, 19]. Notably, BZCs derivatives (albendazole (ABZ), fenbendazole (FBZ), mebendazole (MBZ) etc.) are the most widely used anthelmintics due to their selective binding with colchicine binding domain of β-tubulin [20-28]. Several efforts have been made to explore the role of different functionalities (1-alkyl, aryl, arylalkyl acyl benzimidazoles and hydrogen atom) at N-1/N-3 and C-2 position of the benzimidazole ring (Figure S1) [1, 27, 28]. Structure-activity-relationship (SAR) studies of such compounds indicates that certain types of functional group (*i.e.*, methoxy carbonyl amino and heteroaryl group attached at C-2 position of benzimidazole derivatives through a CO, CHON, CONH, S, SO) [10] improves anthelmintic activities. In spite of these efforts, their bioavailability and resistance remains the main stay problem due to negligence by scientific community, availability of < 1% fund of total pharmaceutical global funds and scarcity of molecular level insight [10].

Owing to the fact that majority of the drugs administrated in the form of salts [17, 20-22, 24-28]; ionic liquids (ILs) (a class of salts/molten salts) can be worthy choice to appraise as an active pharmaceutical ingredients (APIs) [29-39]. Their (ILs) adjustable physicochemical and biological profile makes them pertinent for the uses in various domain such as biotechnology, catalysis, and electrochemistry etc [40-59]. However, clinical applications of ILs as active-pharmaceutical ingredients (APIs) are at premature stage due to their multiple debatable reasons such as toxicity, biochemical and biopharmaceutical properties [40, 41]. At recent times, reasonably, efforts have been made to provide the chemical space for their applications as APIs *via* abating their toxicity, biochemical and biopharmaceutical properties [40, 41]. This can be made by tailoring their solubility, counter anions, N-alkyl chain length and functional group. Possibly the tactic, would reflect their therapeutic application in a greater perspective [40, 41]. It is worth to mention that the

maxim "*the poison is in the dose'*, has encouraged to develop ILs as useful drugs for biomedical applications by minimizing their toxicity [28, 31, 60].

Considering the above mentioned facts and the encouraging outcomes from our previous study (that reveals the vermicidal activity of ILs rely on the nature of N-alkyl side chain and counter anion) [61] we examined to evaluate the vermicidal and cytotoxic activity of the 1-methyl-3-alkylbenzimidazolium and 1-methyl-3-alkylimidazolium derived ILs. Further, the SAR features of fused benzene ring in imidazolium ring of the ILs were also established. Moreover, quantitative-structure-activity-relationship (QSAR) and molecular docking were performed to explicate several bred-in-the-bones factors accountable for their activity and binding patterns of ILs, respectively.

## 2. Experimental

### 2.1. Material and methods

Benzimidazole, 1-methylimidazole, n-ethyl bromide, n-butyl bromide, n-hexyl bromide, n-octyl bromide, and n-decyl bromide, $NaBF_4$ and NaOH were purchased from Sigma-Aldrich and used as received. Albendazole sulfoxide (ABZSO) was purchased from *Hi-media*, India. All the organic solvents were purchased from Avara Synthesis Pvt. Ltd. and R & D Chemicals and distilled prior their usages. $^{1}H$ and $^{13}C$ NMR spectra were recorded using Bruker 400 and 500 MHz spectrometer in appropriate deuterated solvents ($CDCl_3$ and $d_6$-DMSO) and TMS as an internal standard. Mass spectral analysis was accomplished with Agilent Technologies G6520B LCMS (Q-TOF) mass spectrometry with +ESI ionization method.

### 2.2. Synthesis of ionic liquids (ILs)

#### 2.2.1. N-alkylation of Benzimidazole with Methyl bromide

Mixture of Benzimidazole (0.1 mole), 30 mL of 50% of NaOH (*w/v*) and methyl bromide ($CH_3$-Br) (0.11 mole) were stirred at room temperature for 3 minutes (Scheme-1). Afterwards, the reaction mixture was stirred at temperature 40 °C until biphasic layer (one was organic layer and second was aqueous NaOH) appears in round bottom flask. Further, organic layer was extracted from the reaction mixture using $CHCl_3$ ($3 \times 25$ mL). The extract was washed twice with distilled water and sodium sulfate (anhydrous agent), later the organic solvent was evaporated under reduced pressure. Finally, the yellowish color solution was distilled in order to purify and to ensure the synthesis of ILs.

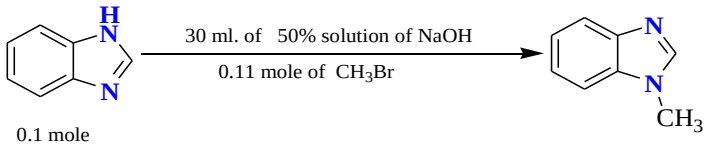


**Scheme 1:** N-alkylation reaction of Benzimidazole with Methyl bromide.

### 2.2.2. Solvent free quaternization of 1-Methylbenzimidzole

In a dry flask 1-methylbenzimidazole or 1-methylimidazole (1.0 equivalent) and 1.2 equivalents of alkyl bromides (*i.e.*, n-ethyl bromide) was added and sealed, heated in an oil bath maintained at 140 °C for 20 minutes, and cooled down to room temperature. Further, the reaction mixture was heated at same temperature (140 °C) for 10 minutes, then cooled down to room temperature (rt). The obtained IL was washed with ethyl acetate ( $(5 \times 25$ mL) to remove the unreacted starting materials), vacuum dried and characterized. The same procedure was applied for the quaternization of the 1-methylbenzimidazole and 1-methylimidazole ring with varying N-alkyl side chain *i.e.*, n-butyl, n-hexyl, n-octyl, and n-decyl bromide. A representative reaction scheme has been given bellow in (Scheme 2, Step-1) [62].

Derivatives of ILs with hydroxide as counter anion [RBZMIM]OH ([EBZMIM]OH, [BBZMIM]OH, [HBZMIM]OH, [OBZMIM]OH, [DBZMIM]OH) and [RMIM]OH ([EMIM]OH, [BMIM]OH, [HMIM]OH, [OMIM]OH, [DMIM]OH) were synthesized by altering the different N-alkyl side chains (*i.e.*, n-$C_2H_5$, n-$C_4H_9$, n-C6H13, n-$C_8H_{17}$ and n-$C_{10}H_{21}$) using anion exchange reaction as per reported procedure [61, 63]. Amberlite resin bearing hydroxide anion was used for above anion transformation reactions. This Amberlite resin bearing hydroxide anion (hydroxide resin) was prepared by stirring Amberlite® IRA-400 chloride resin with 1M NaOH in a round bottom flask for 12 hours. Later, resin with hydroxide anions was obtained by neutralizing their pH by washing with double distilled water, filtered and dried. Moreover, a demonstrative example for the synthesis of [RBZMIM]OH (*i.e.*, [EBZMIM]OH, [BBZMIM]OH, [HBZMIM]OH, [OBZMIM]OH, [DBZMIM]OH) and [RMIM]OH (*i.e.*, [EMIM]OH, [BMIM]OH, [HMIM]OH, [OMIM]OH, [DMIM]OH) derivatives are as follows: 5 g of [RBZMIM]Br and [RMIM]Br IL was dissolved separately in methanol and passed through a column packed with hydroxide resin independently. Subsequently, substrate was concentrated under vacuum followed by vacuum drying leading to 1-methyl-3-alkylimidazolium hydroxide and 1-methyl-3-alkylbenzimidazolium hydroxide derivatives (Scheme 2, Step-2).

Another anion exchange reaction was carried out to achieve IL with boron tetrafluorides as counter anion (IL-$BF_4$) by metathesis reaction as per reported literature with minor modifications (Scheme 2). A demonstrative example for the synthesis of [RMIM]$BF_4$ (*i.e.*, [EMIM]$BF_4$, [BMIM]$BF_4$, [HMIM]$BF_4$, [OMIM]$BF_4$, [DMIM]$BF_4$) and [RBZMIM]$BF_4$ (*i.e.*, [EBZMIM]$BF_4$, [BBZMIM]$BF_4$, [HBZMIM]$BF_4$, [OBZMIM]$BF_4$, [DBZMIM]$BF_4$) in Scheme 2 (step-3) derivatives are as follows: 1:2 ratio of the 1-methyl-3-alkylimidazolium bromide or 1-methyl-3-alkylbenzimidazolium bromide ([RBZMIM]Br) and $NaBF_4$ were added distinctly in to the round bottom flask containing 25mL of methanol and stirred at room temperature for 24 hrs. Afterwards, the salt was removed by filtering the reaction mixture using Whatman filter paper. Further, the filtrate was centrifuge for 10 minutes at 3000rpm to isolate the residual salts. Solvent was evaporated under reduced pressure, vacuum dried and characterized (using $^{1}H$ and $^{13}C$-NMR and mass spectroscopy). The spectral details of the synthesized ILs are provided in the supplementary information Figure S1 to S30.

### 2.3. Evaluation of Vermicidal Activity

*Pheretima posthuma* (Indian earthworm) has been chosen as the model organism for evaluation of vermicidal activity as a model organism due to their physiological and anatomical resemblance with intestinal human parasitic worms. Indian adult earthworm (*Pheretima posthuma*) were collected from wastewater treatment, Management Plant of Golden Temple, Vellore, India and employed for the screening of vermicidal screening. Albendazole sulfoxide (ABZSO) and sterilized distilled water were used as positive control and negative control. The assay was performed according to the literature procedure [61, 64] at four different concentrations (2mM, 4mM, 8mM and 16mM) in a time dependent manner (15, 30, 45, 60, 75, 90, 120 minutes). Their activities were recorded in terms of percentage paralysis and mortality in triplicate at various time interval. Their average value was considered for comparative analysis.

### 2.4. Scanning Electron Microscope (SEM) Analysis

*Sample Preparation***:** ILs treated and untreated earthworms were stored in 2:9:30:59 mixture of acetic acid, formaldehyde, ethanol (95%) and distilled water [65]. Later, morphological study of their skin was performed. Initially, earthworms were taken out from the stored solution and their body parts such as anterior, posterior, dorsal/ ventral part and clitellum were dissected and dried overnight. Afterwards, each part was processed for SEM analysis by following the protocol

reported by Dhvani Jhala *et al.*, [66] Briefly, each body part was fixed with 2% glutaraldehyde in 0.1M sodium cacodylate buffer (pH 7.2) for 1 hr. and later transferred to cacodylate buffer. Next, gradient dehydration was performed by washing samples serially with 30%, 70%, 80%, 90%, 95% and 100% ethanol for 5 to 10 min each. The samples were air-dried, sputter coated with gold-palladium and recorded under SEM (EVO 18, Zeiss Germany) at the distance of 10 mm.

### 2.5. Cytotoxicity Study

Aalamar blue assay was employed to expose the A549 cells against the most active ILs (*i.e.*, [DBZMIM]Br, [DBZMIM]OH and [DBZMIM]$BF_4$) identified during VA to evaluate their level of cytotoxicity. Briefly, the A549 cells were grown in RPMI media supplemented with 10% FBS. At around 70-80% confluency, cells were trypsinized and seeded in 96 well plates as 10000 cells per well. After 24 hours, 4 mM dose of [DBZMIM]Br, [DBZMIM]OH and [DBZMIM]$BF_4$ in media were treated for another 24 hours. As the stocks of compounds were prepared in water, equal volume of water was added to media and incubated in control wells. Again after 24 hours, media was replaced with fresh one containing 10% v/v of the alamar blue solution and incubated for one hour in the dark. Afterwards, absorbance was recorded at 570 nm to evaluate the cell viability using multi-plate reader (SynergyTM H1, BioTek®) [66]. All the experiments were performed in triplicates.

### 2.6. Computational Details

Geometry optimization of 1-methyl-3-alkylbenallynzimidazolium derivatives were carried out at B3LYP/6-311G(d) level of theory level with Conductor-like Polarizable Continuum Solvation Model (CPCM) using Gaussian 09 [67]. Dissimilar guess geometry were obtained by manual positioning of anions with respect to the cationic core of the ILs to estimate the real geometry with minimized total energy [68]. The frequency analysis was also performed at the same level of approximation to ensure the structures were at global minima. The details of the optimized guess geometries have been given in electronic supplementary information (ESI) Table S1.

### 2.7. Generation of QSAR model

The fifteen 1-methyl-3-alkylbenzimidazolium derive ILs with varying N-alkyl chains (n-$C_2H_5$ to n-$C_{10}H_{21}$) and three different anions ($Br^-$, $BF_4^-$ and $OH^-$) were considered for the QSAR using

Discovery Studio v4.0 [62]. Computationally, it is very challenging to mimic ILs real geometrical features due to the presence of characteristic interaction between the $[C]^+[X]^-$($X^+$ = cations, and $X^-$= anions) [68, 69]. For this reason, density functional theory (DFT) based descriptors of the cations and anions were separately computed and used in QSAR model development (refer TableS3) [68]. Notably, the critical electronic and solvation effects were considered during the generation of independent variables (descriptors). Also, the average percentage mortality (at 4mM concentration) were converted to $log_{10}$ *[% mortality]* and considered as the dependent variable [70][67].

Multiple Linear Regression (MLR) technique was applied for the selection of optimal combination of descriptors (Table S2) [71]. The following criteria was considered for the MLR based modelling *viz* number of components 20, number of nearest neighbors 20, smoothness parameter 0.5, decorrelation method was Pearson, max. correlation 0.99, model development finger print FCFP_2, dynamic smoothing factor 0.5, fingerprint distance function Tanimato, Max OPS fingerprint Bits 1000 and total number of variables were thirty.

The quality of MLR model was measured based on $r^2$ and RMSE, as governed by the following equations.

$$r^2 = 1 - \frac{\sum(Y_{obs} - Y_{cal})^2}{\sum(Y_{obs} - \bar{Y}_{obs})^2} \qquad (1)$$

Whereas, $Y_{obs}$ stand for the observed activity, $Y_{cal}$ is the model-derived calculated response and $\bar{Y}_{obs}$ is the average of the observed response value. RMSE (Root Mean Square Error (RMSE) is a measure of how close the data is around the line of best fit) was also examined.

$$RMSE = \sqrt{\frac{1}{N} \times \sum(y_{obs} - y_{cal})^2} \qquad (2)$$

Where, N is number of components.

### 2.8. Molecular docking study

Molecular docking study was performed using the DFT optimized ligand structures of cationic part ($[EBZMIM]^+$, $[BBZMIM]^+$, $[HBZMIM]^+$, $[OBZMIM]^+$, $[DBZMIM]^+$) and a 3D-homology receptor model of *H. contortus* β-tubulin bound to Albendazole sulfoxide [72] (PDB entry: 1OJ0) [73]. Initially, protein preparation and binding site were defined by selecting the grid box size of 8 Å using *receptor preparation wizard*. Discovery Studio (DS) v4.0 program was employed to dock cationic head groups in highly dynamic tubulin environment using flexible docking method.

It uses the ChiFlex and CDOCKER algorithm [74] to generate the side chains (active site) conformations and to dock the low energy conformations of cationic group in to the flexible binding pockets respectively [75]. Refinement of the active side residues was made by ChiRotor algorithm [74]. The simulated annealing (SA) approach was applied to minimize the poses in various restrained steps using the parameters such as heating temperature (500 K), cooling temperature (300 K), conformer generation method (BEST), grid extension (8.0 Å) and maximum conformation (10). Also, SIFt binding pattern [76-78] of β-tubulin inhibitors distribution of colchicine binding domain [79] and the interactions patterns of the dock poses have been exemplified in 2D format using ligand-receptor interaction map. The present *in-silico* procedure is an advancement over the current methods [77] for computational assessment of ILs.

### 2.9. ADME/T assessment

The pharmacological properties of the 1-methyl-3-alkylbenzimidazolium derived ILs were evaluated by the *in-silico* predictions to measure the biological regimen. Absorption, Distribution, Metabolism, Excretion and Toxicity (or ADME/T) of the ILs were assessed by considering the subsequent features: Aqueous Solubility, Blood Brain Barrier (BBB), Hepatotoxicity, Intestinal Absorption, Plasma Protein Binding (PPB) properties (refer Table S3) [80-86].

## 3. Results and discussions

Our previous findings indicates that vermicidal activities of the ILs depends on the nature of varying alkyl chains and counter anions ($Br^-$and $OH^-$) [61]. We further pursuit research in this line and evaluate the vermicidal activities of 1-methyl-3-alkylimidazolium and 1-methyl-3-alkylbenzimidazolium derived ILs, with diverse alkyl chains (*i.e.*, n-$C_2H_5$, n-$C_4H_9$, n-$C_6H_{13}$ n-$C_8H_{17}$ and n-$C_{10}H_{21}$, substituted at N-3 position of imidazolium ring) and different cationic and anionic ($Br^-$, $OH^-$, $BF_4^-$) combinations.

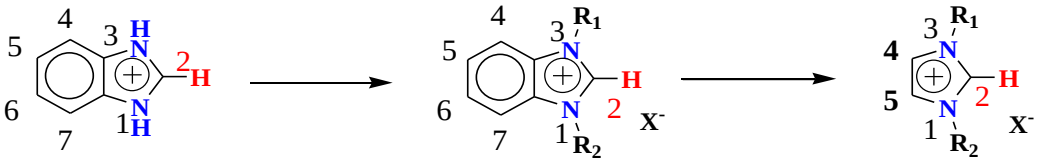


Where, $R_1$= -$CH_3$, $R_2$ = -$C_2H_5$, -$C_4H_9$, -$C_6H_{13}$, -$C_8H_{17}$, -$C_{10}H_{21}$ and X = Br/ or OH/ $BF_4$

**Figure 1:** List of imidazolium and benzimidazolium salts.

### 3.1. Vermicidal Activities of ionic liquids (ILs)

The synthesized compounds (as mentioned in Scheme 2) were tested for the vermicidal activities as a function of percentage paralysis and mortality. Percentage paralysis and mortality of the *1-methyl-3-alkylbenzmidazolium bromide* derivatives (*i.e.*, [EBZMIM]Br, [BBZMIM]Br, [HBZMIM]Br, [OBZMIM]Br and [DBZMIM]Br), *1-methyl-3-alkylbenzmidazolium boron tetrafluoride* derivatives (*i.e.*, [EBZMIM]$BF_4$, [BBZMIM]$BF_4$, [HBZMIM]$BF_4$, [OBZMIM]$BF_4$ and [DBZMIM]$BF_4$), and *1-methyl-3-alkylbenzmidazolium hydroxide* derivatives (*i.e.*, [EBZMIM]OH, [BBZMIM]OH, [HBZMIM]OH, [OBZMIM]OH and [DBZMIM]OH), *1-methyl-3-alkylimidazolium bromide* (*i.e.*, [EMIM]Br, [BMIM]Br, [HMIM]Br, [OMIM]Br and [DMIM]Br), *1-methyl-3-alkylmidazolium boron tetrafluoride* derivatives (*i.e.*, [EMIM]$BF_4$, [BMIM]$BF_4$, [HMIM]$BF_4$, [OMIM]$BF_4$ and [DMIM]$BF_4$), and *1-methyl-3-alkylimidazolium hydroxide* derivatives ([EMIM]OH, [BMIM]OH, [HMIM]OH, [OMIM]OH and [DMIM]OH) and *Albendazole sulfoxides* (ABZSO) were evaluated at four different concentrations in a time dependent manner. The detailed information of the vermicidal activities (VAs) is given in supplementary information (Figure S31 to S45). Based on the results and arguments mentioned in ESI, it have been comprehended that ILs VA depends on doses and nature of N-alkyl side chain (or hydrophobicity). Average percentage VA (as function of percentage paralysis and mortality) at 4mM concentration of 1-methyl-3-alkylimidazolium and 1-methyl-3-alkylbenzimidaolium derivatives have been considered and compared to elucidate the effects of different anions ($Br^-$, $OH^-$ and $BF_4^-$), cationic core and structure activity relationship (SAR) of the ILs.

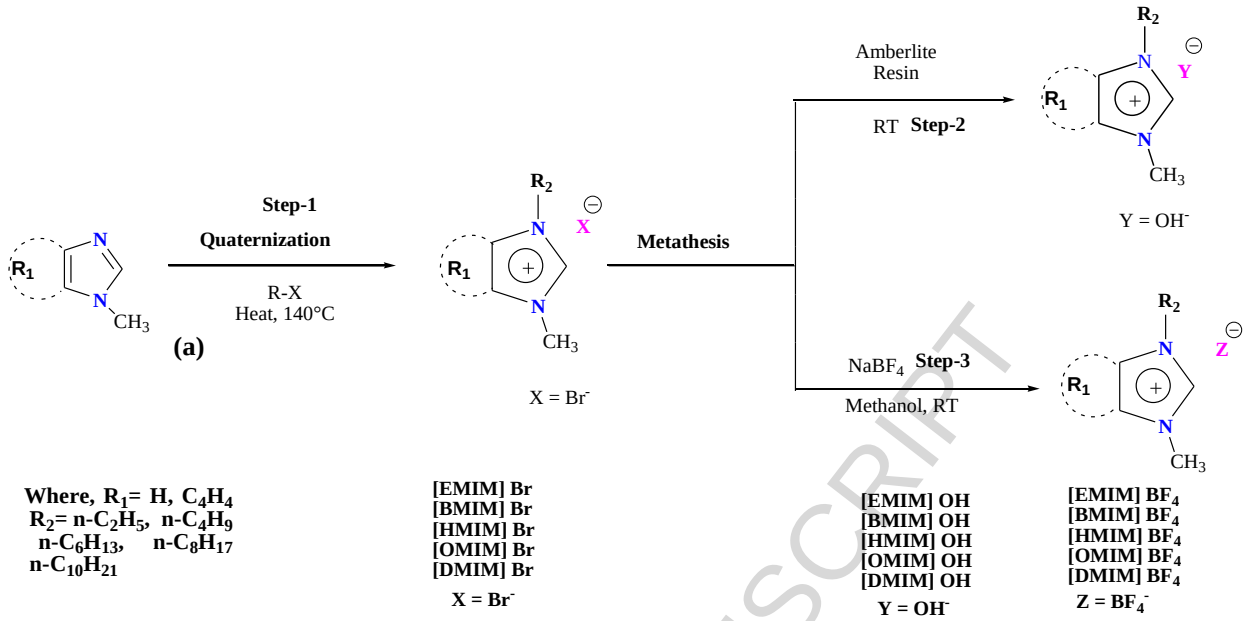


**Scheme 2:** General scheme for the synthesis of 1-methyl-3-alkylimidazolium and 1-methyl-3-alkylbenzimidazolium derived ILs.

**Structure activity relationship (SAR) of the tested ILs with vermicidal activity (VA)**

Herein, effects of different anions and fused benzene ring at C-4 and C-5 position of the imidazolium ring of IL were perceived by considering the VAs of tested ILs (at 4mM conc.) as given in Figure 2. ILs (1-methyl-3-alkylimidazolium or [RMIM] and 1-methyl-3-alkylbenzimidaolium [RBZMIM] derivatives) showed very competitive percentage paralysis (**Figure 2a**) with respect to the same N-alkyl side chain containing two different cationic core ($[RMIM]^+$ and [RBZMIM]+) except [EMIM]Br. Conversely, a significant variation in percentage mortality of the ILs can be observed with alteration of the different anions ($Br^-, OH^-$ and $BF_4^-$) and N-alkyl chains with fixed cationic core (**Figure 2b**). From, Figure 2b the difference in VAs of 1-methyl-3-alkylimidazolium and 1-methyl-3-alkylbenzimidazolium derivatives having the same N-alkyl side-chain and different anions ($Br^-, OH^-$ and $BF_4^-$) can be clearly noticed. Hence, it can be comprehend that ILs-OH showed slightly better mortality than IL-$BF_4$, IL-Br and ABZSO (refer **Figure 2b**). However, it can be conclude that IL-OH exhibits significant activities then IL-BF4, IL-Br and ABZSO, due to the high hydrophobic and lipophilic ratio. Furthermore, Figure 2 deciphers that ILs [RBZMIM] OH/ Br/ $BF_4$ derivatives shows better activities than 1-methyl-3-alkylimidazolium derive ILs and standard drug (ABZSO). Likewise, it can be noticed that ABZSO exhibits better and competitive percentage paralysis than ILs *i.e.*, [EMIM] and [BMIM] Br/ $BF_4$/ OH (**Figure 2a**). On the other hand, ILs [EMIM] and [BMIM] Br/or$BF_4$/or OH and [HBMIM]$BF_4$

shows very competitive mortality with ABZSO (**Figure 2b**). It may be possible due to the lesser hydrophobic factors in comparison to ABSO. Also, these findings supports the fact that "majority of the drugs exist in salt form" [72, 87-90]. Besides, fusion of benzene ring in imidazolium ring of the IL affects the VA in greater extents compared to 1-methyl-3-alkylimidazolium derivatives. A possible explanations for this trend can be provided from the earlier literature reports [72, 87-90]. BZCs derivatives can efficiently binds to colchicine domain of β-tubulin monomer and thereby block the microtubule formation. Also, they suppress the β-tubulin polymerase enzyme, as a consequence lead to decrease in glucose level (due to the exhaustion of glycogen levels/storage) and finally results in the death of the parasite [91-97]. Further, in quest to provide better insight to the experimental findings QSAR and molecular docking approach have been employed. For that, the most active series of compounds ([RBZMIM]Br/or OH/or $BF_4$) have been considered.

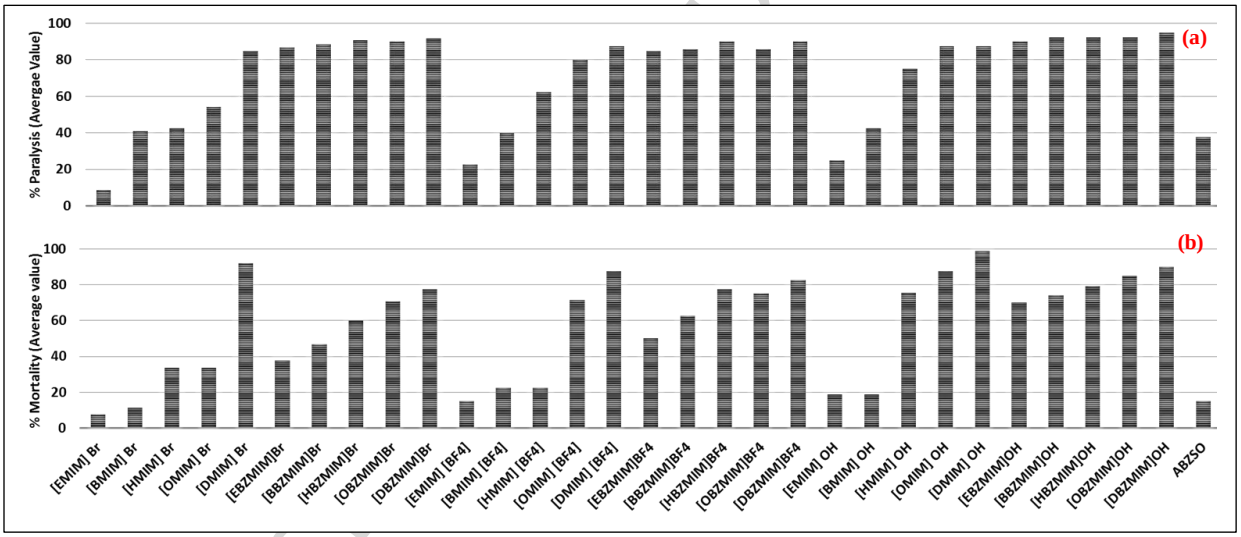


**Figure 2:** Comparison of %paralysis **(a)** and %mortality **(b)** of 1-methyl-3-alkylimidazolium and 1-methyl-3-alkylbenzimidazolium derivatives (IL-Br, IL-$BF_4$ and IL-OH) containing three different anions and ABZSO (as standard drug).

### 3.2. SEM Analysis:

The images of tegumental surfaces of untreated (as positive control) earthworm have been given in Figure 3 mouth (**a**), anus (**b**) dorsal (**c-e**) and ventral (**f-h**) side surfaces appeared undamaged. Mouth part (Figure b) and anus part (Figures d) recorded at high magnifications for better resolution that showed the normal and undamaged prostomium (it covers the mouth of earthworm, helps in dwell the soil and function as sensor). Further, dorsal part (**c-e**) and ventral part (**f-h**) was recorded at 200, 300X and 1,000KX (Figure 3), clearly indicates the presence of grooves with

setae (helps in locomotion of the earthworm) marked by red arrow (in Figure 3 **e** and **h**) were found as in normal and healthy earthworm morphology.

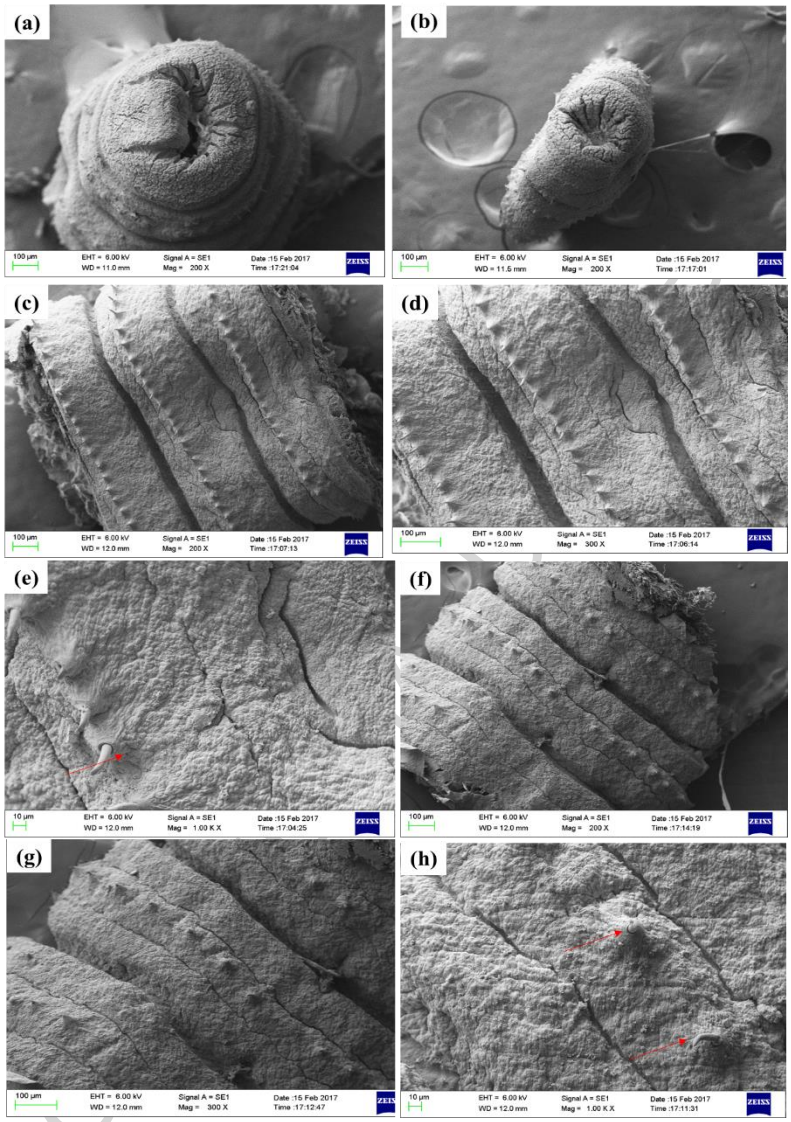


**Figure 3:** Scanning electron microscopy of the different parts of the untreated or uninfected Indian earthworm (*P. posthuma*) to study the morphological changes. (**a**) showing normal and regular arrangements of mouth part recorded at 200X (**b**) showing no morphological change in anus part recorded at 200 X (**c, d**) displaying normal and proper arrangements of grooves and spines (shown by red arrow) present on the dorsal tegumental surface recorded at 200X, 300 X and 1,000 KX and (**e, f**) ventral healthy tegumental surface with presence of clear grooves and spines (shown by red arrow), recorded at 200X, 300 X and 1,000 K. The alternation of the teguments (helps in define the shape of earthworms body, moisten the body wall, respiration as well as muscle contraction and relaxations) on the earthworm skin morphology treated with ILs were analyzed by scanning electron microscopy (SEM) Figure 4 (**g-h**).

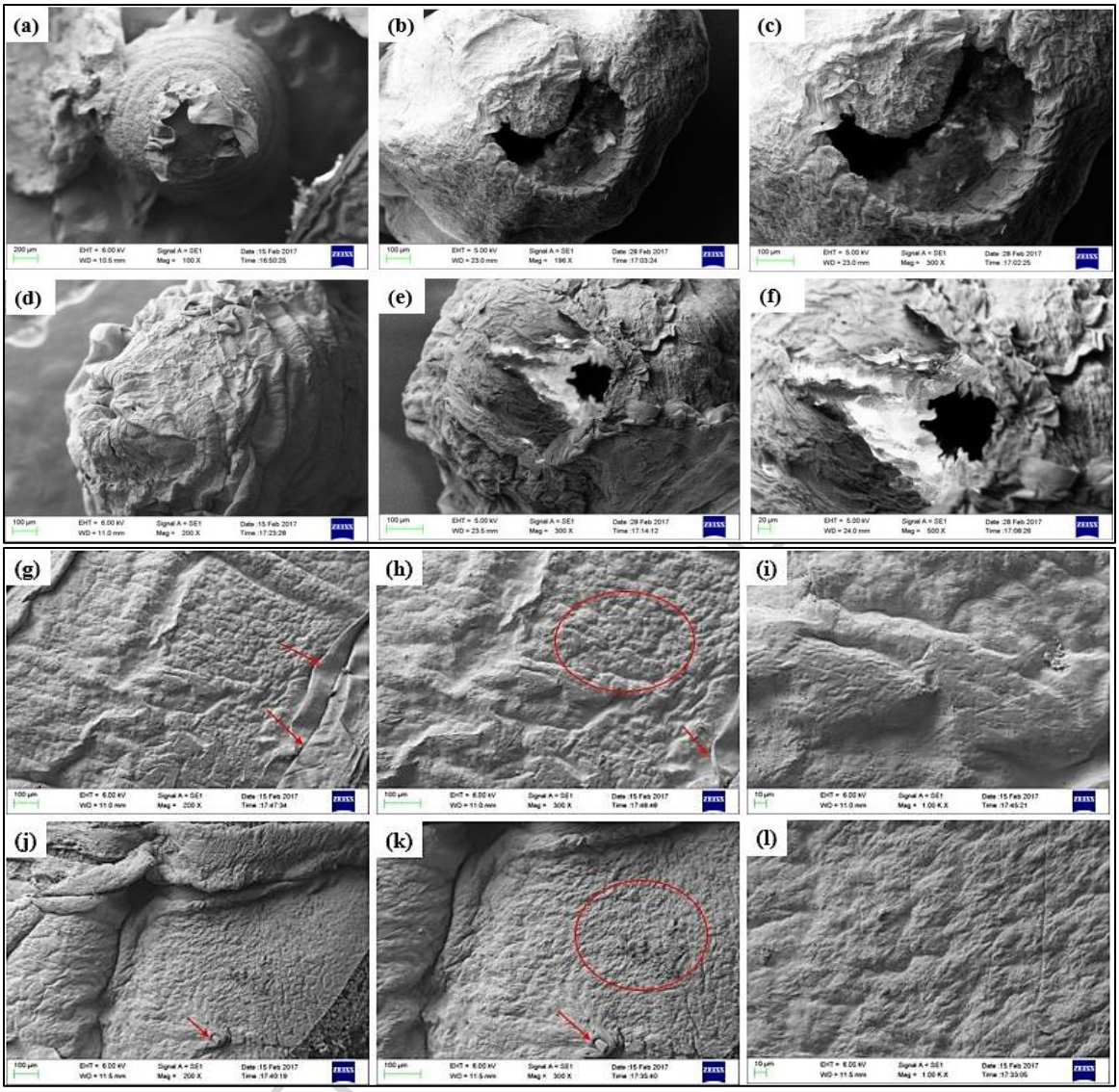


**Figure 4:** Scanning electron microscopy of the different parts of the ILs treated Indian earthworm (*P. posthuma*) to study the morphological changes. (**a-c**) showing damaged and ruptured skin around the mouth part recorded at 200X, 300X and 1,000X, (**d-f**) damaged, ruptured and swelled skins around anus part recorded at 200X, 300X and 1,000X, (**g-i**) ruptured skins (marked with red arrows) and no absence of grooves and spines on the dorsal tegumental surface recorded at 200X, 300 X and 1,000 KX, and (**j-l**) evidently showing ruptured skins (marked with red arrows) and no absence of grooves and spines (blunted spine) on the ventral tegumental surface recorded at 200X, 300 X and 1,000 KX.

Figure 4 (**a-f**) illustrates the damaged and swelled tegumental surfaces on their mouth and anus part. Similar observations can be perceived from Figure 4 of (**g-i**) and (**j-l**) recorded for dorsal and ventral section respectively showing damaged tegumental surfaces, and the folded skin (damaged and ruptured) marked with red arrows shown in Figure 4 **g** and **h**. Moreover, image (Figure 4 **h**)

circled in red color is showing flashes of dorsal section of earthworms, and the image encircled in red color display a small pore in the earthworm flashes. Also, images recorded for their ventral section (**h, i**) are showing absence of setae's (that help in locomotion of earthworm, made up of *chitin*) or annular row. Moreover, images recorded for ventral section showing blunt spines marked with red arrow (in Figure 4 **j** and **k**). The area encircled in red color (shown in Figure 4 **k**) display the flashes with blunted setae. Their damaged tegumental surface and setae leads to stop all vital functions of earthworm (such as respiration, absorption, secretion, protection as well as their movement as well) which leads to death of the test organism.

These findings can be supported by the originally proposed biochemical mode of action for the clinically available anthelmintic drugs [87, 91-93, 97]. They suppress the β-tubulin polymerase enzyme and triggers the consumption of glucose that results in lowering of glucose level [87, 91-93, 97]. Also, increasing hydrophobicity index with increase in N-alkyl side chain and polar surface area (IL-OH > IL-$BF_4$ > IL-Br) damages the cell wall and cutaneous layer of the worm results in leakage of body fluids that leads to death of worms. This encouraged to evaluate the binding mode of ILs against the β-tubulin structure using the molecular docking approach.

### 3.3. Cytotoxicity evaluation of Ionic Liquids (ILs)

Cytotoxicity results presented in Figure 5 describes the different cytotoxic levels of the test compounds (most active ILs). [DBZMIM]Br and [DBZMIM]$BF_4$ showed lowest levels of cytotoxicity, with 58% of cell survival and [DBZMIM]OH showed highest level of cytotoxicity with, 2% of cell survival. Furthermore, these results are self-explanatory that cytotoxicity of these ILs also depends on the nature of the anions with fixed cations. Also, this finding suggest that ILs toxicity can be controlled by tailoring the different anionic and cationic combinations, it provides balance between their toxicity and drug-likeness properties to develop as APIs.

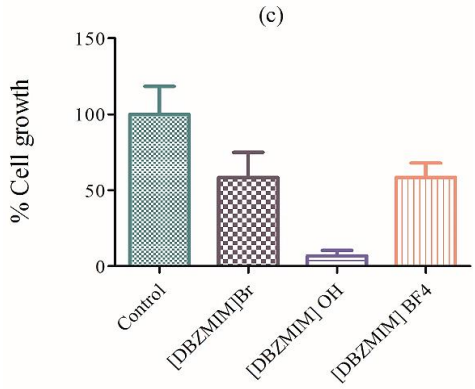


**Figure 5:** Cytotoxicity assay of [DBZMIM]Br, [DBZMIM]OH and [DBZMIM]$BF_4$ on A549 cells after 24 hours. The data shows decrease in the % cell growth as a function of cytotoxic level of the compounds.

### 3.4. Geometry Optimization

The geometries of 15 ILs were optimized at B3LYP/6-311G(d) level of theory using Gaussian 09 program [67]. Out of the various delineated structure of each IL, the lowest energy geometry without imaginary frequency was selected (Table S1). Results of the optimized structures revealed that the distance between the anionic moieties and C-2 positioned hydrogen atom of the benzimidazolium rings varies by altering the different anion ($Br^-, OH^-$ and $BF_4^-$). With increase in bulkiness of the anion with fixed cation, the distance between the anionic moieties and C-2 positioned hydrogen atom varied. They can be arranged in ascending order of their average distance considered between the C-2 hydrogen and anionic moieties, which are as follows: $OH^-$ $(0.9843\ Å) > BF_4^-(2.3652\ Å) > Br^-$ $(2.5362\ Å)$.

**Quantitative structure activity relationship (QSAR) Modelling**

QSAR based studies were performed *via* utilizing quantum mechanical based descriptors to identify the role of cation and anion for their vermicidal activity of the synthesized ILs. Based on the RMSE and the regression statistics, we selected the model equation with *a_CP* (Chemical potential of anion), *a_LUMO* (Lowest unoccupied molecular orbital of anion) and *c_FPSA* (Fractional polar surface area of anion) descriptors. Multiple Linear Regression model equation is as follows:

$$\boldsymbol{Log10(activity) = 2.355 + 0.008082 * [a\_CP] - 0.7414 * [a\_LUMO] - 10.88 * [c\_FPSA]}$$

The closeness of the respective variables (*a_LUMO, a_CP, c_FPSA*) with the observed values in terms of their numeric differences can be perceived from Table 1. It can be said that in case of the minimum value (Min.) and standard deviation (SD) of *a_LUMO* (Min. 0.107 and SD. 0.088) *and c_FPSA* (Min. 0.026 and SD. 0.007) have showed closeness with the experimental number (Min. 1.574 and SD. 0.103), while *a_CP* (Min. -1.770 and SD. 1.167) displayed large deviation from the experimental number (Table 1). Therefore, these descriptors can be represented in order of influencing the observed activity *i.e., a_LUMO* > *c_FPSA* > *a_CP*. It was evident to note that these descriptors contributed to the %mortality and thus supported our experimental findings that account the effects of anion exchange on vermicidal activities of ionic liquids and fused benzene ring at imidazolium derive ionic liquids. The list of descriptors have been given in the Table 1.

**Table 1:** List of quantum mechanical descriptors used in MLR model

| ***Descriptors*** | ***Min.** | ***Max.** | **Mean** | *** SD[b]** | **X[a]** |
|---|---|---|---|---|---|
| *a_CP* | -1.770 | 1.076 | -0.267 | 1.167 | 0.008 |
| *a_LUMO* | 0.107 | 0.319 | 0.201 | 0.088 | -0.741 |
| *c_FPSA* | 0.026 | 0.046 | 0.034 | 0.007 | -10.884 |
| *activity* | 1.574 | 1.954 | 1.828 | 0.103 | |
| *Min. (Minimum), Max. (Maximum), SD[b] (Standard Deviation), X[a] (Regression coefficient of descriptors) | | | | | |

Detailed statistics of the developed quantum mechanical based MLR model have been given in Table 2, as the square root of correlation coefficient ($r^2$) and predicted correlation coefficient ($r^2_{adjusted}$). The obtained MLR statistics with significant regression coefficient ($r^2$) 0.88, and RMSE 0.034, signify the model with good fitness ability. Additionally, the $r^2_{adjusted}$ is a better measure of the ratio than $r^2$ that avoids the over-parameter value for the MLR was 0.857. It is clearly indicating that the variation and correlation in the whole data is in good agreement.

The correlation graph plotted between predicted activities (on the Y-axis) *Vs* observed % mortality (on the X-axis) in Figure 6 shows significant correlation with $r^2$= 88.33% for the MLR model. Thus, the predicted QSAR model can be used to predict new *lead* molecule against helminths incorporating these factors. It can be noticed that the predicted values are in good agreement with the experimental values. The observed % mortality and predicted values for the whole data set of the MLR models are listed in Table S3 (Supplementary data).

**Table 2:** Details of the statistics of the developed quantum mechanical based GFA model

| Sl No. | Statistic | Value |
|---|---|---|
| **1** | $N$ | 15 |
| **2** | $r$ | 0.942 |
| **3** | $r^2$ | 0.887 |
| **4** | $r^2_{predicted}$ | 0.759 |
| **5** | $r^2_{adjusted}$ | 0.857 |
| **6** | RMSE residual error | 0.034 |
| **7** | RMS residual error (cross-validation) | 0.005 |

**N** = No. of components; $r^2$= Regression coefficient; $\boldsymbol{r^2_{adjusted}}$= Square root of adjusted $r^2$= correlation coefficient; $\boldsymbol{r^2_{predicted}}$ **= square root of p**redicted correlation coefficient, **RMSE** = Root Mean Square Error; $\boldsymbol{q^2}$= Cross-validation, r = correlation coefficient

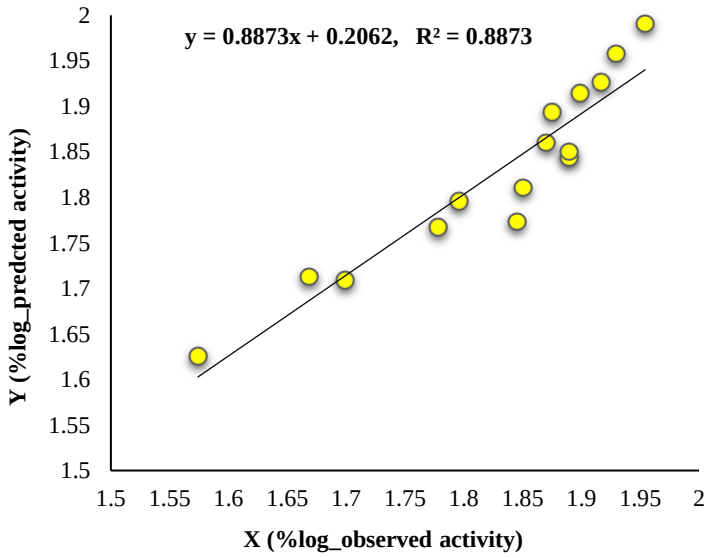


**Figure 6:** Correlation plot of observed (X-axis) versus predicted activities (Y-axis) by MLR.

### 3.5. Molecular Docking study

In continuation to our previous studies based on the evaluation of anthelmintic activities of the ILs and alternate binding sites (*zone 1*, *2* and *3*) [61, 77], we have attempted to identify binding site of the synthesized compounds. For that, molecular docking of 1-methyl-3-alkylbenzimidazolium derived cationic head groups *viz.* $[EBZMIM]^+$, $[BBZMIM]^+$, $[HBZMIM]^+$, $[OBZMIM]^+$ and $[DBZMIM]^+$ was performed to investigate the binding interactions [76, 79]. The resulting 3D Dock poses of the ligand-receptor complexes have been given in the Figure 7. The cationic part of the ligands highlighted in red color (in ball and CPK form) with interacting amino acids (Figure 7).

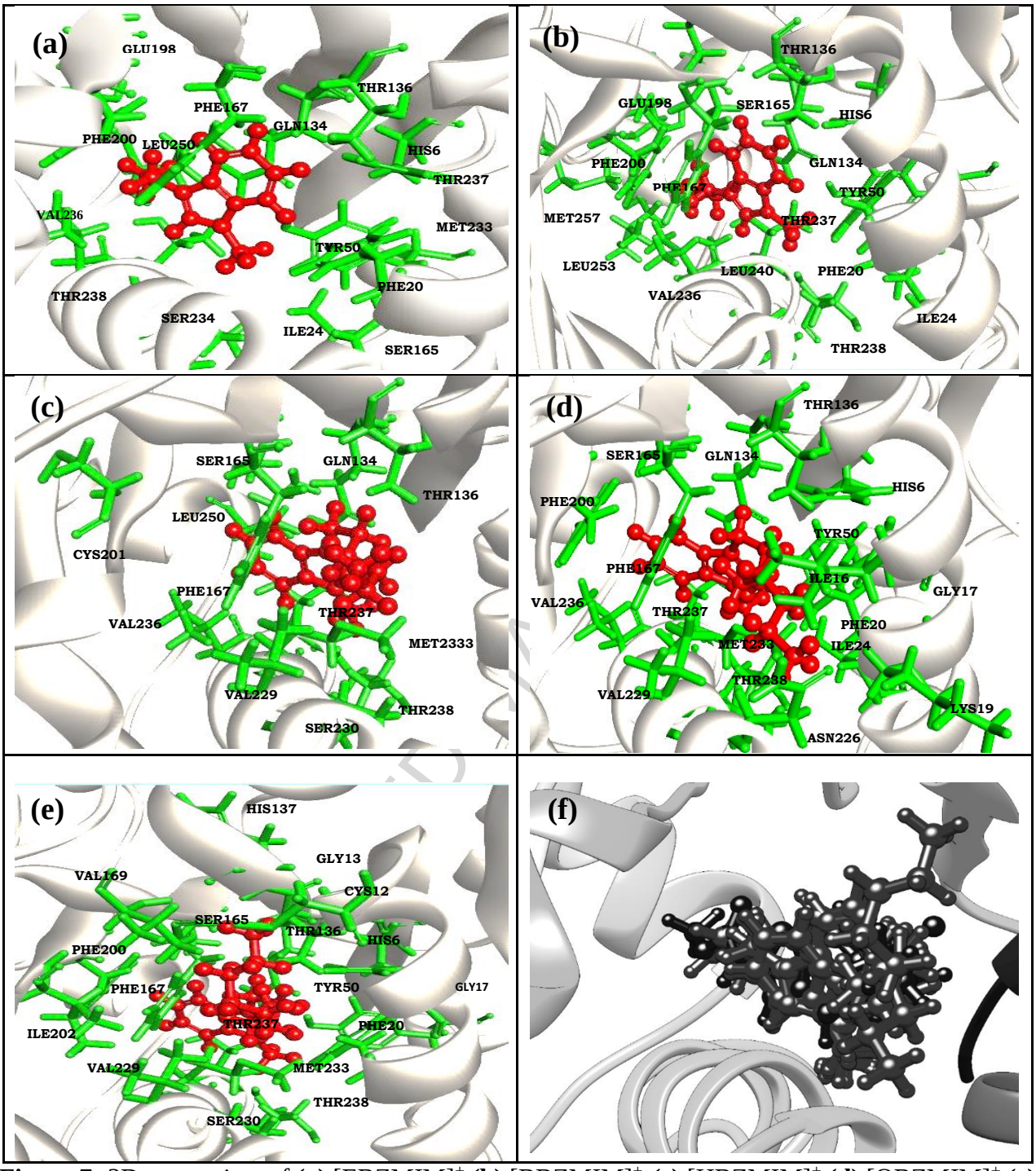


**Figure 7:** 3D poses view of **(a)** $[EBZMIM]^+$ **(b)** $[BBZMIM]^+$ **(c)** $[HBZMIM]^+$ **(d)** $[OBZMIM]^+$ **(e)** $[DBZMIM]^+$ and **(f)** $[RBZMIM]^+$ of β-tubulin inhibitors on the *H. contortus* β-tubulin model.

Moreover, the details of the interacting amino acids have been listed in Table 3. It was found that amino acids *viz.* HIS6, MET233, GLN134, PHE200, PHE167, and SER165 were consistent in

each ligand and receptor complex (Table 3**)**. In general, ligand-receptor complex possess four major types of interactions van der Waal, л-л, hydrophobic and electrostatic interactions.

**Table 3:** Docking score and interacting amino acids of [RBZMIM] derive ILs

| ILs | Docking Score (Kcal/mol) | Interacting Amino acids |
|---|---|---|
| **[EBZMIM]+** | -20.568 | ILE24, PHE20, SER234, PHE167, SER165, THR238, PHE200, LEU250, GLU198, TYR50, MET233, HIS6, THR136, THR237, GLN134, VAL236 |
| **[BBZMIM]+** | -23.7665 | ILE24, SER234, PHE20, THR238, PHE167, HIS6, THR237, VAL236, PHE200, THR136, LEU250, SER166, SER165, LEU240, ALA254, GLU198, LEU253, MET257, TYR50, MET233, GLN134 |
| **[HBZMIM]+** | -23.9864 | LEU250, VAL236, THR237, THR238, ILE24, SER165, PHE200, ILE16, PHE167, ILE16, THR136, VAL229, SER234, PHE20, SER230, GLN134, MET233, TYR50 |
| **[OBZMIM]+** | -25.6676 | VAL236, THR237, SER165, HIS6, ILE24, THR238, PHE167, THR136, VAL229, SER230, SER234, PHE200, ILE16, GLY17, PHE20, ASN226, LYS19, TYR50, MET233, GLN134 |
| **[DBZMIM]+** | -28.5137 | HIS6, CYS12, GLY13, PHE20, THR136, GLY17, GLN134, SER165, VAL169, LEU250, VAL229, SER230, ILE202, PHE200, THR237, TYR50, VAL236, MET233, MET236, PHE167 |

*Green color residues shows van der Wall interactions, Light blue color shows л-л interaction, amino acid residues in pink color shows interaction with positively charged nitrogen of imidazolium ring and residues in orange color shows non-classical H-bond interaction

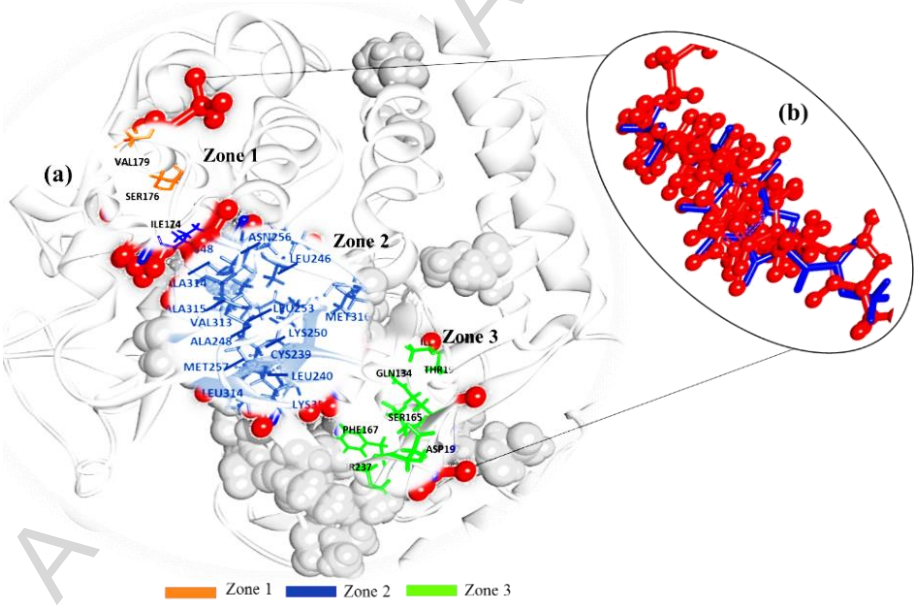


**Figure 8: (a)** The amino acids participating in the interaction zones *viz.*1 to 3 (colchicine binding domain) are represented in the line view (orange -zone-1, blue -zone-2, light green -zone-3), identified according to SIFt patterns, **(b)**. Superimposed structures of $[RBZMIM]^+$ in red color with reference ligands benzimidazole sulfoxide (blue color) in colchicine binding domain.

The residue HIS6 interact with the positively charged nitrogen of imidazolium ring. Also, PHE167, MET233 and PHE200 were engaged in л-л interactions, whereas, GLN134 form non-classical H-bond interaction. Moreover, SER165 interact with hydrogen atom present at C-4 position in the imidazolium ring (Table S47). It was further observed (Figure 8) that all five ligands were considerably superimposed over the reference ligand (ABZSO). Interpretation of interactions zones in colchicine binding domain by SIFt pattern reveals that all the docked ligands overlap in *zone-1* to *3* as highlighted in Figure 8 (*with three different colors: orange -zone-1, blue -zone-2, light green -zone-3*). Notably, major part of the ligands binds in *zone-2* (highlighted in blue color) in align to our previous finding [77].

Results have shown that, anthelmintic activity increases with increase in alkyl chain and magnitude of positive charge on the quaternary nitrogen of the imidazolium ring. It can be articulated from the graph (Figure 9 *plotted for comparing the experimentally observed percentage mortality with docking score*) that with increase in alkyl length (ranging from *n-ethyl* to *n-decyl*), docking score were also increases (in negative magnitude). These findings are complementary to the observed trends of the percentage paralysis and mortality. This study indicates that hydrophobic region, positively charged quaternary nitrogen of the 1-methyl-3-alkylbenzimidazolium rings are the key factors in influencing the anthelmintic activities.

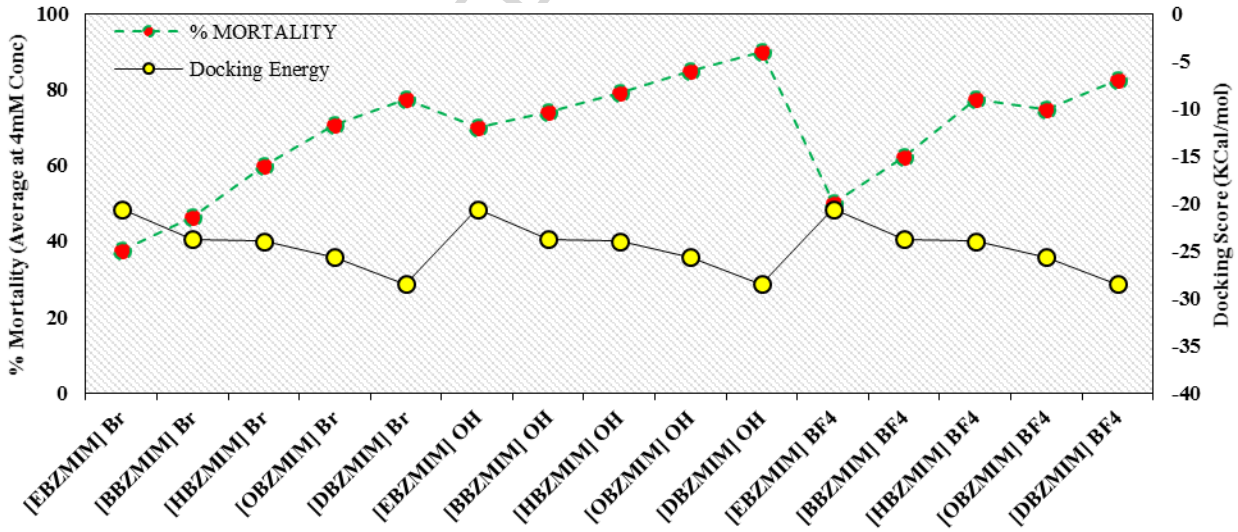


**Figure 9:** The correlation plots of the average percent mortality of earthworms (in different time interval at 4mM conc. in red color) and the docking score (in dotted black color) of the RBZMIM-Br /or $BF_4$/or OH.

### 3.6. ADME/T assessment

It provides a qualitative idea about the absorption, distribution, metabolism, excretion and toxicity in the pharmacokinetics of the employed ILs [98, 99]. The assessment was carried out by considering the various ADME/T descriptors, given in Table S3. All fifteen (15) molecules qualified the ADMET profiling test (pharmacokinetics, pharmacodynamics and toxicity study) with default standards as implemented in DS. Figure 10 (For 95% and 99% confidence ellipse biplot), clearly shows that majority of the compounds follows the bioavailability criteria and are probably show drug-likeness features [100]. However, molecules outside of the absorption (95%) confidence ellipse biplot ([DBZMIM] Br/OH/$BF_4$), does not possess drug-likeness properties (**Table S3**) and considered as unreliable. That may possible due their higher hydrophobic factors (presence of n-decyl alkyl chain at N3 positions of benzimidazolium ring.

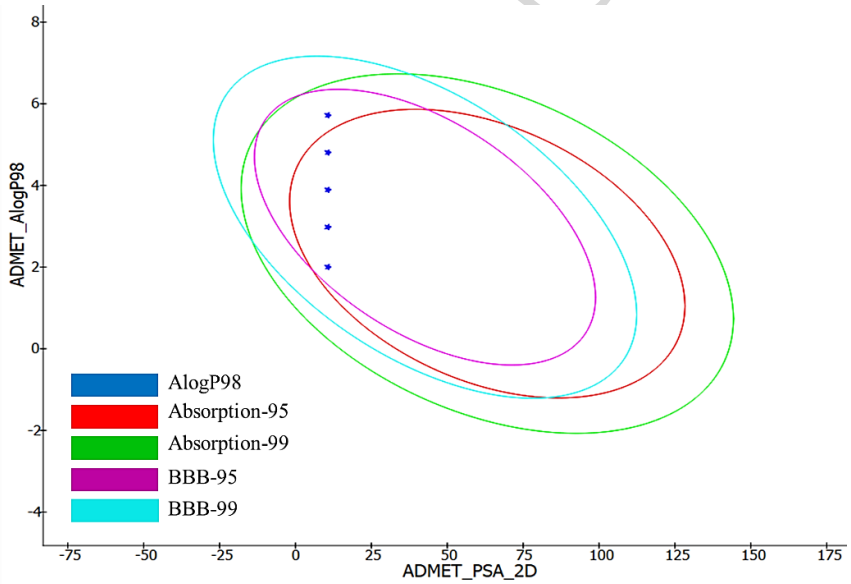


**Figure 10:** ADMET 2D description plot of the polar surface area (X-axis) *vs* LogP for 1-methyl-3-alkylbenzimidazolium derived ILs, showing 95% and 99% confidence limit ellipses corresponding to the Blood Brain Barrier and Intestinal Absorption models.

**Conclusion:**

Herein, we report that VA and cell viability of ionic salts depends on the nature of N-alkyl side chain, anionic moieties, varying charge on quaternary nitrogen, lipophilicity and types of cationic core fused with imidazolium ring. ILs having hydroxide ($OH^-$) as counter anion shows significant activities over $BF_4^-$, $Br^-$ and ABZSO. Similarly, cell viability study proved that ionic salts can be tuned to provide chemical space to develop them as novel APIs. SEM analysis advocates that increasing hydrophobicity index and polar surface area (IL-OH > IL-$BF_4$ > IL-Br) damages the cell wall and cutaneous layer of the test organism. It leads to leakage of body fluids, thereby allowed them to cross the cell membrane and interrupt the vital activities of the worms that causes to death of the test organism. Also, this can be supported form the proposed biochemical mode of action for the clinically available anthelmintic drugs [87, 91-93, 97]. Further, structure-activity-relationship (SAR) study showed that 1-methyl-3-alkylbenzimidazolium derived salts exhibits better activity than 1-methyl-3-alkylimidazolium derived salts. It is possible, due to high binding affinity of the 1-methyl-3-alkylbenzimidazolium derived salts towards the colchicine binding domain of the β-tubulin protein.

These experimental observations supported by QSAR study described that descriptors *a_CP*, *a_LUMO* of the anions and *c_FPSA* of the cations are responsible factors for the activities of 1-methyl-3-alkylbenzimidazolium derivatives. From this, it can be conclude that $OH^-$ (as counter anion) increases the polar surface area (PSA) of the cationic head, subsequently $BF_4^-$ and $Br^-$ anion (as have been given in above para). Additionally, ligand-receptor interaction studies of the cationic heads of the 1-methyl-3-alkylbenzimdiazolium derivatives suggests that they majorly binds in *zone-2* of the colchicine binding domain of the β-tubulin protein; hydrophobic region and positively charged quaternary nitrogen of the 1-methyl-3-alkylbenzimidazolium rings are the key factors in influencing the anthelmintic activities. Further, *in-silico* ADME/T assessment study confirms that all fifteen compounds passes the ADME and toxicity profiling test. However, these current findings open a new landscape for these ionic salts advancement as a novel potential anthelmintic *leads* and for other biomedical applications.

**Acknowledgements:** Prabodh Ranjan thanks financial support from University Grants Commission (UGC), Govt. of India. Mr. Mohd Athar acknowledges generous support from the Department of Science and Technology (DST), Govt. of India as Doctoral INSPIRE Fellowship. Dr. Prakash Chandra Jha also would like to thanks Science and Engineering Research Board (SERB) for providing start-up grants and Central University of Gujarat for providing basic computational facilities.

**Author contributions:** Prabodh Ranjan, Mohd Athar, Kari Vijayakkrishna and Prakash C. Jha designed the research problem. Prabodh Ranjan and Mohd Athar performed the calculations and interpret the results.

**Conflict of Interest:** Authors have no personal, financial or non-financial conflicts of interest.

**References:**

[1] H. Hoste, F. Jackson, S. Athanasiadou, S.M. Thamsborg, S.O. Hoskin, The effects of tannin-rich plants on parasitic nematodes in ruminants, Trends in parasitology 22(6) (2006) 253-261.
[2] S. Plotkin, D.J. Diemert, J.M. Bethony, P.J. Hotez, Hookworm vaccines, Clinical Infectious Diseases 46(2) (2008) 282-288.
[3] T. Eguale, G. Tilahun, A. Debella, A. Feleke, E. Makonnen, Haemonchus contortus: in vitro and in vivo anthelmintic activity of aqueous and hydro-alcoholic extracts of Hedera helix, Experimental parasitology 116(4) (2007) 340-345.
[4] T. Eguale, G. Tilahun, A. Debella, A. Feleke, E. Makonnen, In vitro and in vivo anthelmintic activity of crude extracts of Coriandrum sativum against Haemonchus contortus, Journal of Ethnopharmacology 110(3) (2007) 428-433.
[5] D. Davyt, W. Entz, R. Fernandez, R. Mariezcurrena, A.W. Mombrú, J. Saldana, L. Domínguez, J. Coll, E. Manta, A New Indole Derivative from the Red Alga Chondria atropurpurea. Isolation, Structure Determination, and Anthelmintic Activity 1, Journal of natural products 61(12) (1998) 1560-1563.
[6] D.E. Akiyoshi, L.M. Weiss, X. Feng, B.A. Williams, P.J. Keeling, Q. Zhang, S. Tzipori, Analysis of the β-Tubulin Genes from Enterocytozoon bieneusi Isolates from a Human and Rhesus Macaque, Journal of eukaryotic microbiology 54(1) (2007) 38-41.
[7] S. Parida, V.J. Patro, U.S. Mishra, L. Mohapatra, S. Sannigrahi, Anthelmintic potential of crude extracts and its various fractions of different parts of Pterospermum acerifolium Linn, Inter J Pharma Sci Rev Res 1(Suppl 2) (2010) 107-11.
[8] R.G. Mali, A.A. Mehta, A review on anthelmintic plants, (2008).
[9] N. Anand, S. Sharma, Approaches to design and synthesis of antiparasitic drugs, Elsevier1997.
[10] V.E. Relf, H.E. Lester, E.R. Morgan, J.E. Hodgkinson, J.B. Matthews, Anthelmintic efficacy on UK Thoroughbred stud farms, International journal for parasitology 44(8) (2014) 507-514.
[11] J.C. Van De Steene, W.E. Lambert, Validation of a solid-phase extraction and liquid chromatography–electrospray tandem mass spectrometric method for the determination of nine basic pharmaceuticals in wastewater and surface water samples, Journal of chromatography A 1182(2) (2008) 153-160.

[12] M. Zrnčić, M. Gros, S. Babić, M. Kaštelan-Macan, D. Barcelo, M. Petrović, Analysis of anthelmintics in surface water by ultra high performance liquid chromatography coupled to quadrupole linear ion trap tandem mass spectrometry, Chemosphere 99 (2014) 224-232.
[13] R. Prichard, Anthelmintic resistance, Veterinary parasitology 54(1-3) (1994) 259-268.
[14] F. Nchu, J. Githiori, L.J. McGaw, J.N. Eloff, Anthelmintic and cytotoxic activities of extracts of Markhamia obtusifolia Sprague (Bignoniaceae), Veterinary parasitology 183(1) (2011) 184-188.
[15] R. Dahiya, D. Pathak, Synthetic studies on novel benzimidazolopeptides with antimicrobial, cytotoxic and anthelmintic potential, European journal of medicinal chemistry 42(6) (2007) 772-798.
[16] S. Sharma, V. Agarwal, S. Dubey, R. Iyer, N. Anand, R. Chatterjee, S. Chandra, A. Sen, STUDIES IN POTENTIAL FILARICIDES. 19. SYNTHESIS OF 1-METHYL-4-SUBSTITUTEDCARBONYLPIPERAZINES AS DIETHYLCARBAMAZINE ANALOGS, INDIAN JOURNAL OF CHEMISTRY SECTION B-ORGANIC CHEMISTRY INCLUDING MEDICINAL CHEMISTRY 26(8) (1987) 748-751.
[17] A.E. Mourad, D.S. Wise, L.B. Townsend, Synthesis of imidazo [1, 2-b] pyridazines: Fenbendazole, oxifenbendazole analogs and related derivatives, Journal of heterocyclic chemistry 30(5) (1993) 1365-1372.
[18] J. Baggot, Q. McKellar, The absorption, distribution and elimination of anthelmintic drugs: the role of pharmacokinetics, Journal of Veterinary Pharmacology and Therapeutics 17(6) (1994) 409-419.
[19] Y. Bansal, O. Silakari, The therapeutic journey of benzimidazoles: a review, Bioorganic & medicinal chemistry 20(21) (2012) 6208-6236.
[20] R. Chatterjee, N. Fatma, V. Agarwal, S. Sharma, N. Anand, Comparative antifilarial efficacy of the N-oxides of diethylcarbamazine and two of its analogues, Tropical medicine and parasitology: official organ of Deutsche Tropenmedizinische Gesellschaft and of Deutsche Gesellschaft fur Technische Zusammenarbeit (GTZ) 40(4) (1989) 474-475.
[21] E.F. Elslager, S. Perricone, F.H. Tendick, Antifilarial agents. I. Effects of 4-[(7-chloro-4-quinolyl) amino]-. alpha.-(mono-and dialkylamino)-o-cresols and related compounds against Litomosoides carinii in gerbils, Journal of medicinal chemistry 12(6) (1969) 965-969.
[22] S. Sharma, Advances in the treatment and control of tissue-dwelling helminth parasites, Progress in Drug Research/Fortschritte der Arzneimittelforschung/Progrès des recherches pharmaceutiques, Springer1986, pp. 473-547.
[23] S. Sharma, Treatment of Filariasis—Diethylcarbamazine and Its Congeners, Pharmaceutical research 3(2) (1986) 75-80.
[24] M. Go, T. Ngiam, A.S. Wan, Synthesis of some novel amodiaquine analogs as potential antimalarial and antifilarial compounds, Journal of medicinal chemistry 24(12) (1981) 1471-1475.
[25] P. Wadia, N. Anand, Studies in Potential Filaricides: Part III-Synthesis of Homopiperazine Analogues of Antifilarial Piperazines, (1958).
[26] J. Reinertson, P. Thompson, Effects of JGS-11o (N, N-diethyl-4-methyUi-diaza-cycloheptaae-i-carboxamide, hydrochloride) against fiiariasis in cotton rats, Antibiotics & Chemotherapy 1(5) (1955) 566-570.
[27] P.A. Sturm, M. Cory, D.W. Henry, J. McCall, J. Ziegler, Antifilarial agents. 3-Aminopyrrolidine and 1, 4-diazabicyclo [3.2. 1] octane derivatives as analogs of diethylcarbamazine, Journal of medicinal chemistry 20(10) (1977) 1333-1337.
[28] A. Bousvaros, B. Mueller, Thalidomide in gastrointestinal disorders, Drugs 61(6) (2001) 777-787.
[29] V. Kumar, S.V. Malhotra, Study on the potential anti-cancer activity of phosphonium and ammonium-based ionic liquids, Bioorganic & medicinal chemistry letters 19(16) (2009) 4643-4646.
[30] S.V. Malhotra, V. Kumar, A profile of the in vitro anti-tumor activity of imidazolium-based ionic liquids, Bioorganic & medicinal chemistry letters 20(2) (2010) 581-585.
[31] S.V. Malhotra, V. Kumar, C. Velez, B. Zayas, Imidazolium-derived ionic salts induce inhibition of cancerous cell growth through apoptosis, MedChemComm 5(9) (2014) 1404-1409.

[32] C. Agatemor, K.N. Ibsen, E.E. Tanner, S. Mitragotri, Ionic Liquids for Addressing Unmet Needs in Healthcare, Bioengineering & Translational Medicine (2018).
[33] H.D. Williams, L. Ford, S. Lim, S. Han, J. Baumann, H. Sullivan, D. Vodak, A. Igonin, H. Benameur, C.W. Pouton, Transformation of Biopharmaceutical Classification System Class I and III Drugs Into Ionic Liquids and Lipophilic Salts for Enhanced Developability Using Lipid Formulations, Journal of pharmaceutical sciences 107(1) (2018) 203-216.
[34] T.E. Sintra, K. Shimizu, S.P. Ventura, S. Shimizu, J.C. Lopes, J.A. Coutinho, Enhanced dissolution of ibuprofen using ionic liquids as catanionic hydrotropes, Physical Chemistry Chemical Physics 20(3) (2018) 2094-2103.
[35] J.-H. An, J.-M. Kim, S.-M. Chang, W.-S. Kim, Application of ionic liquid to polymorphic design of pharmaceutical ingredients, Crystal growth & design 10(7) (2010) 3044-3050.
[36] S.H. KP, M.S. Thayyil, M. Binesh, S. Deshpande, V.K. Rajan, Molecular dynamics in amorphous pharmaceutically important protic ionic liquid–benzalkonium chloride, Journal of Molecular Liquids (2017).
[37] Z. Yan, L. Ma, S. Shen, J. Li, Studies on the interactions of some small biomolecules with antibacterial drug benzethonium chloride and its active pharmaceutical ingredient ionic liquid (API-IL) benzethonium L-proline at varying temperatures, Journal of Molecular Liquids 255 (2018) 530-540.
[38] A.R.C. Duarte, A.S.D. Ferreira, S. Barreiros, E. Cabrita, R.L. Reis, A. Paiva, A comparison between pure active pharmaceutical ingredients and therapeutic deep eutectic solvents: Solubility and permeability studies, European Journal of Pharmaceutics and Biopharmaceutics 114 (2017) 296-304.
[39] M. Malamatari, K.M. Taylor, S. Malamataris, D. Douroumis, K. Kachrimanis, Pharmaceutical nanocrystals: production by wet milling and applications, Drug discovery today (2018).
[40] R. Ferraz, L.C. Branco, C. Prudencio, J.P. Noronha, Ž. Petrovski, Ionic liquids as active pharmaceutical ingredients, ChemMedChem 6(6) (2011) 975-985.
[41] W.L. Hough-Troutman, M. Smiglak, S. Griffin, W.M. Reichert, I. Mirska, J. Jodynis-Liebert, T. Adamska, J. Nawrot, M. Stasiewicz, R.D. Rogers, Ionic liquids with dual biological function: sweet and anti-microbial, hydrophobic quaternary ammonium-based salts, New Journal of Chemistry 33(1) (2009) 26-33.
[42] W.L. Hough, M. Smiglak, H. Rodríguez, R.P. Swatloski, S.K. Spear, D.T. Daly, J. Pernak, J.E. Grisel, R.D. Carliss, M.D. Soutullo, The third evolution of ionic liquids: active pharmaceutical ingredients, New Journal of Chemistry 31(8) (2007) 1429-1436.
[43] M.S. Sitze, E.R. Schreiter, E.V. Patterson, R.G. Freeman, Ionic liquids based on FeCl3 and FeCl2. Raman scattering and ab initio calculations, Inorganic chemistry 40(10) (2001) 2298-2304.
[44] N.K. Kaushik, P. Attri, N. Kaushik, E.H. Choi, Synthesis and antiproliferative activity of ammonium and imidazolium ionic liquids against T98G brain cancer cells, Molecules 17(12) (2012) 13727-13739.
[45] K. Maddali, V. Kumar, C. Marchand, Y. Pommier, S.V. Malhotra, Biological evaluation of imidazolium- and ammonium-based salts as HIV-1 integrase inhibitors, MedChemComm 2(2) (2011) 143-150.
[46] M.R. Cole, M. Li, B. El-Zahab, M.E. Janes, D. Hayes, I.M. Warner, Design, Synthesis, and Biological Evaluation of β-Lactam Antibiotic-Based Imidazolium-and Pyridinium-Type Ionic Liquids, Chemical biology & drug design 78(1) (2011) 33-41.
[47] J. Pernak, P. Chwała, Synthesis and anti-microbial activities of choline-like quaternary ammonium chlorides, European journal of medicinal chemistry 38(11) (2003) 1035-1042.
[48] J. Pernak, I. Goc, I. Mirska, Anti-microbial activities of protic ionic liquids with lactate anion, Green Chemistry 6(7) (2004) 323-329.
[49] J. Pernak, J. Kalewska, H. Ksycińska, J. Cybulski, Synthesis and anti-microbial activities of some pyridinium salts with alkoxymethyl hydrophobic group, European journal of medicinal chemistry 36(11) (2001) 899-907.

[50] M. Ghavre, O. Byrne, L. Altes, P.K. Surolia, M. Spulak, B. Quilty, K.R. Thampi, N. Gathergood, Low toxicity functionalised imidazolium salts for task specific ionic liquid electrolytes in dye-sensitised solar cells: a step towards less hazardous energy production, Green Chemistry 16(4) (2014) 2252-2265.
[51] G.G. Mandawad, R.D. Kamble, S.V. Hese, R.A. More, R.N. Gacche, K.M. Kodam, B.S. Dawane, An efficient synthesis of isoxazoline libraries of thiophene analogs and its antimycobacterial investigation, Medicinal Chemistry Research 23(10) (2014) 4455-4463.
[52] P.N. Dube, S.S. Bule, S.N. Mokale, M.R. Kumbhare, P.R. Dighe, Y.V. Ushir, Synthesis and Biologic Evaluation of Substituted 5-methyl-2-phenyl-1H-pyrazol-3 (2H)-one Derivatives as Selective COX-2 Inhibitors: Molecular Docking Study, Chemical biology & drug design 84(4) (2014) 409-419.
[53] M. Zhao, Y. Cui, J. Yu, S. Xu, X. Guo, Combined use of hydroxypropyl-β-cyclodextrin and ionic liquids for the simultaneous enantioseparation of four azole antifungals by CE and a study of the synergistic effect, Journal of separation science 37(1-2) (2014) 151-157.
[54] P. Khloya, P. Kumar, A. Mittal, N.K. Aggarwal, P.K. Sharma, Synthesis of some novel 4-arylidene pyrazoles as potential antimicrobial agents, Organic and medicinal chemistry letters 3(1) (2013) 9.
[55] J. Feder-Kubis, K. Tomczuk, The effect of the cationic structures of chiral ionic liquids on their antimicrobial activities, Tetrahedron 69(21) (2013) 4190-4198.
[56] M. Messali, Eco-friendly synthesis of a new class of pyridinium-based ionic liquids with attractive antimicrobial activity, Molecules 20(8) (2015) 14936-14949.
[57] N. Ferlin, M. Courty, S. Gatard, M. Spulak, B. Quilty, I. Beadham, M. Ghavre, A. Haiß, K. Kümmerer, N. Gathergood, Biomass derived ionic liquids: synthesis from natural organic acids, characterization, toxicity, biodegradation and use as solvents for catalytic hydrogenation processes, Tetrahedron 69(30) (2013) 6150-6161.
[58] P. Ranjan, B.S. Kitawat, M. Singh, 1-Butylimidazole-derived ionic liquids: synthesis, characterisation and evaluation of their antibacterial, antifungal and anticancer activities, RSC Advances 4(96) (2014) 53634-53644.
[59] Y. Yu, Y. Nie, Toxicity and antimicrobial activities of ionic liquids with halogen anion, Journal of Environmental Protection 2(03) (2011) 298.
[60] G.B. Vogelsang, E.R. Farmer, A.D. Hess, V. Altamonte, W.E. Beschorner, D.A. Jabs, R.L. Corio, L.S. Levin, O.M. Colvin, J.R. Wingard, Thalidomide for the treatment of chronic graft-versus-host disease, New England Journal of Medicine 326(16) (1992) 1055-1058.
[61] K.P. Charan, P. Ranjan, K. Manojkumar, N. Pothanagandhi, P.C. Jha, V.M. Khedkar, A. Sivaramakrishna, K. Vijayakrishna, Evaluation of imidazolium-based ionic liquids towards vermicidal activity: in vitro & in silico studies, RSC Advances 5(92) (2015) 75415-75424.
[62] S.V. Dzyuba, R.A. Bartsch, Efficient synthesis of 1-alkyl (aralkyl)-3-methyl (ethyl) imidazolium halides: Precursors for room-temperature ionic liquids, Journal of Heterocyclic Chemistry 38(1) (2001) 265-268.
[63] I. Dinarès, C.G. de Miguel, A. Ibáñez, N. Mesquida, E. Alcalde, Imidazolium ionic liquids: A simple anion exchange protocol, Green Chemistry 11(10) (2009) 1507-1510.
[64] E. Ajaiyeoba, P. Onocha, O. Olarenwaju, In vitro anthelmintic properties of Buchholzia coriaceae and Gynandropsis gynandra extracts, Pharmaceutical Biology 39(3) (2001) 217-220.
[65] J. de Moraes, Antischistosomal natural compounds: present challenges for new drug screens, Current topics in tropical medicine, InTech2012.
[66] D. Jhala, H. Rather, R. Vasita, Polycaprolactone–chitosan nanofibers influence cell morphology to induce early osteogenic differentiation, Biomaterials science 4(11) (2016) 1584-1595.
[67] M. Frisch, Guassian 09, Gaussian, Wallingford, CT, There is no corresponding record for this reference (2009).
[68] N.L. Mai, C.K. Kim, B. Park, H.-J. Park, S.H. Lee, Y.-M. Koo, Prediction of cellulose dissolution in ionic liquids using molecular descriptors based QSAR model, Journal of Molecular Liquids 215 (2016) 541-548.

[69] C.-W. Cho, S. Stolte, Y.-S. Yun, Comprehensive approach for predicting toxicological effects of ionic liquids on several biological systems using unified descriptors, Scientific reports 6 (2016).
[70] Accelrys Discovery Studio version 4.0, Accelrys San Diego, USA (2016). http://accelrys.com/products/collaborative-science/biovia-discovery-studio/
[71] M. Fernández, J. Caballero, QSAR models for predicting the activity of non-peptide luteinizing hormone-releasing hormone (LHRH) antagonists derived from erythromycin A using quantum chemical properties, Journal of molecular modeling 13(4) (2007) 465-476.
[72] M.W. Robinson, N. McFerran, A. Trudgett, L. Hoey, I. Fairweather, A possible model of benzimidazole binding to β-tubulin disclosed by invoking an inter-domain movement, Journal of Molecular Graphics and Modelling 23(3) (2004) 275-284.
[73] F.C. Bernstein, T.F. Koetzle, G.J. Williams, E.F. Meyer, M.D. Brice, J.R. Rodgers, O. Kennard, T. Shimanouchi, M. Tasumi, The protein data bank, The FEBS Journal 80(2) (1977) 319-324.
[74] V.Z. Spassov, L. Yan, P.K. Flook, The dominant role of side-chain backbone interactions in structural realization of amino acid code. ChiRotor: A side-chain prediction algorithm based on side-chain backbone interactions, Protein Science 16(3) (2007) 494-506.
[75] G. Wu, D.H. Robertson, C.L. Brooks, M. Vieth, Detailed analysis of grid-based molecular docking: A case study of CDOCKER—A CHARMm-based MD docking algorithm, Journal of computational chemistry 24(13) (2003) 1549-1562.
[76] Z. Deng, C. Chuaqui, J. Singh, Structural interaction fingerprint (SIFt): a novel method for analyzing three-dimensional protein− ligand binding interactions, Journal of medicinal chemistry 47(2) (2004) 337-344.
[77] P. Ranjan, S.P. Kumar, V. Kari, P.C. Jha, Exploration of interaction zones of β-tubulin colchicine binding domain of helminths and binding mechanism of anthelmintics, Computational Biology and Chemistry 68 (2017) 78-91.
[78] J.r. Koska, V.Z. Spassov, A.J. Maynard, L. Yan, N. Austin, P.K. Flook, C. Venkatachalam, Fully automated molecular mechanics based induced fit protein− ligand docking method, Journal of chemical information and modeling 48(10) (2008) 1965-1973.
[79] A. Massarotti, A. Coluccia, R. Silvestri, G. Sorba, A. Brancale, The tubulin colchicine domain: a molecular modeling perspective, ChemMedChem 7(1) (2012) 33-42.
[80] A. Cheng, K.M. Merz, Prediction of aqueous solubility of a diverse set of compounds using quantitative structure− property relationships, Journal of medicinal chemistry 46(17) (2003) 3572-3580.
[81] W.J. Egan, G. Lauri, Prediction of intestinal permeability, Advanced drug delivery reviews 54(3) (2002) 273-289.
[82] W.J. Egan, K.M. Merz, J.J. Baldwin, Prediction of drug absorption using multivariate statistics, Journal of medicinal chemistry 43(21) (2000) 3867-3877.
[83] R.G. Susnow, S.L. Dixon, Use of robust classification techniques for the prediction of human cytochrome P450 2D6 inhibition, Journal of chemical information and computer sciences 43(4) (2003) 1308-1315.
[84] S.L. Dixon, K.M. Merz, One-dimensional molecular representations and similarity calculations: methodology and validation, Journal of medicinal chemistry 44(23) (2001) 3795-3809.
[85] J.R. Votano, M. Parham, L.M. Hall, L.H. Hall, L.B. Kier, S. Oloff, A. Tropsha, QSAR Modeling of Human Serum Protein Binding with Several Modeling Techniques Utilizing Structure− Information Representation, Journal of medicinal chemistry 49(24) (2006) 7169-7181.
[86] X. Xia, E.G. Maliski, P. Gallant, D. Rogers, Classification of kinase inhibitors using a Bayesian model, Journal of medicinal chemistry 47(18) (2004) 4463-4470.
[87] P. Köhler, The biochemical basis of anthelmintic action and resistance, Elsevier, 2001.

[88] L.M. MacDonald, A. Armson, R.A. Thompson, J.A. Reynoldson, Characterisation of benzimidazole binding with recombinant tubulin from Giardia duodenalis, Encephalitozoon intestinalis, and Cryptosporidium parvum, Molecular and biochemical parasitology 138(1) (2004) 89-96.
[89] L.C. Davidse, Benzimidazole fungicides: mechanism of action and biological impact, Annual review of phytopathology 24(1) (1986) 43-65.
[90] R. Aguayo-Ortiz, O. Méndez-Lucio, J.L. Medina-Franco, R. Castillo, L. Yépez-Mulia, F. Hernández-Luis, A. Hernández-Campos, Towards the identification of the binding site of benzimidazoles to β-tubulin of Trichinella spiralis: insights from computational and experimental data, Journal of Molecular Graphics and Modelling 41 (2013) 12-19.
[91] V. Barrère, L. Alvarez, G. Suarez, L. Ceballos, L. Moreno, C. Lanusse, R.K. Prichard, Relationship between increased albendazole systemic exposure and changes in single nucleotide polymorphisms on the β-tubulin isotype 1 encoding gene in Haemonchus contortus, Veterinary parasitology 186(3) (2012) 344-349.
[92] E. Chambers, E.M. Hoey, A. Trudgett, I. Fairweather, D.J. Timson, Binding of serum albumin to the anthelmintic drugs albendazole, triclabendazole and their sulphoxides, Veterinary parasitology 171(1) (2010) 172-175.
[93] D. Gottschall, V. Theodorides, R. Wang, The metabolism of benzimidazole anthelmintics, Parasitology Today 6(4) (1990) 115-124.
[94] E. Lacey, The role of the cytoskeletal protein, tubulin, in the mode of action and mechanism of drug resistance to benzimidazoles, International journal for parasitology 18(7) (1988) 885-936.
[95] E. Lacey, Mode of action of benzimidazoles, Parasitology Today 6(4) (1990) 112-115.
[96] R. Martin, Modes of action of anthelmintic drugs, The Veterinary Journal 154(1) (1997) 11-34.
[97] R. McCracken, W. Stillwell, A possible biochemical mode of action for benzimidazole anthelmintics, International journal for parasitology 21(1) (1991) 99-104.
[98] T. Hou, X. Xu, ADME evaluation in drug discovery, Journal of molecular modeling 8(12) (2002) 337-349.
[99] C. Remya, K.V. Dileep, I. Tintu, E.J. Variyar, C. Sadasivan, In vitro inhibitory profile of NDGA against AChE and its in silico structural modifications based on ADME profile, Journal of molecular modeling 19(3) (2013) 1179-1194.
[100] C. Hansch, A. Leo, D. Hoekman, Exploring QSAR, ACS Professional Reference Book, ACS: Washington DC 269 (1995).

Graphical abstract

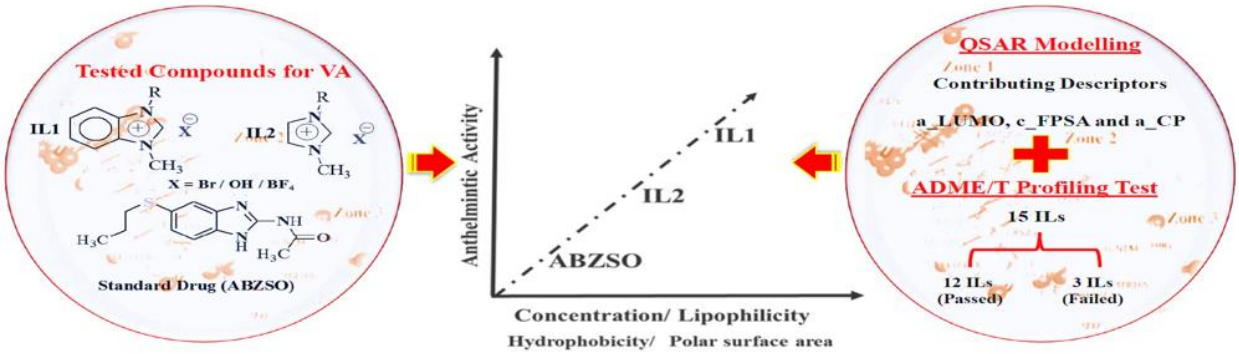

## Highlights:

- **Vermicidal activities of thirty imidazolium derived ILs were studied**
- **IL-OH shows better activities then IL-$BF_4$, IL-Br and ABZSO**
- **Activities depends on nature of N-alkyl chain length, anions, hydrophobic factors, lipophilicity**
- **Descriptors *i.e. c_FPSA of cation*, *a_HOMO* and *a_LUMO* of anions are accountable the ILs activity**
- **80% of the tested ILs pass the ADME/T profiling test**